JOURNAL OF MATERIALS SCIENCE 31 (1996) 1997–2007

Microstructures and room temperature mechanical properties of NiAl prepared by high pressure reaction sintering

TIANYI CHENG
Metal Materials Section, Seventh Dept., Beijing Institute of Technology, PO Box 327, Beijing 100081, People's Republic of China and International Center for Materials Physics, Academia Sinica, Shengyang 110015, People's Republic of China

The microstructures and room temperature compressive mechanical properties of a near-stoichiometric NiAl manufactured by a new high pressure reaction sintering (HPRS) process are investigated. Applying a very high uniaxial pressure (2 GPa) leads to considerable lowering of the sintering temperature and reducing the hold time gives NiAl with a good sintering density. The HPRS NiAl consists of β-NiAl with a B2 structure containing a high density of dislocations, 3.5×10^9 cm^{-2}, and very fine Al_2O_3 particles. The NiAl exhibits quite high true compressive strain, 14.5%, and a reasonably high yield strength, 526 MPa. The effects of employing the high pressure in the HPRS process on the reaction sintering, microstructures and mechanical properties of the NiAl are studied.

1. Introduction

More and more interest has been recently focused on the intermetallic NiAl with a B2 ordered structure which shows unique properties [1, 2]. NiAl is expected to be applied as a high temperature structural material, at or above 900 °C. However, some problems, such as poor ductility at room temperature and low creep strength at elevated temperatures, have not been satisfactorily solved for its application. Moreover, although the very high melting temperature (1638 °C) of NiAl is an advantage for its high temperature structural application, it also results in severe cracking and core-related problems in the manufacture of the single-crystal cast or traditionally cast NiAl [3]. Hence, much effort, such as alloying with other elements [4], refining microstructure size [5], introducing a softer phase [6, 7] and adding appropriate ceramic particles [8, 9], for directly improving the mechanical properties of the NiAl, and various studies in its manufacturing processes and its composites, have been carried out. The processes applied include Bridgman single crystal growth [4], rapid solidification [9], mechanical alloying [10–12], plasma deposition [13] and powder metallurgy [14, 15]. The preliminary results have indicated that the application of the new manufacturing processes is helpful in improving the microstructures and mechanical properties of NiAl. In these processes, the powder metallurgical approach is attractive in overcoming the difficulties in the manufacture of cast NiAl. The powder metallurgical process also is a necessary step following some other processes, such as rapid solidification and mechanical alloying. Hence, how to preserve the improved properties of the NiAl obtained by applying the previous processes is an important issue in the application of the powder metallurgical approach.

Stoloff and co-workers [14, 15] have done much initial work in applying the powder metallurgical approach to the fabrication of NiAl and other intermetallics. The powder metallurgical approaches which have been employed to manufacture these intermetallics mainly include reaction sintering (RS), hot pressure reaction sintering (hot pressure RS) and reaction hot isostatic pressing (RHIP) [13]. The NiAl intermetallics with a good sintering density prepared by hot pressing RS (the pressure employed usually 30–50 MPa) or RHIP (the pressure about 170 MPa) normally have to be heated to about 1200 °C and held there for about 1–2 h, in addition to sometimes employing the hot extrusion process or annealing at high temperature. Grain growth thus readily occurs and the grain size of the products is normally large, 30–50 μm [13], which is disadvantageous to the mechanical properties of NiAl at ambient temperature.

Dynamic compact processes [16], such as explosive compaction applied for consolidation of rapidly solidified powders, can be used to avoid grain growth but inhomogeneous microstructures of the products affect their mechanical properties. On the other hand, high hydrostatic pressure has, for a long time, been applied to study phase transformations [17], synthesis of diamond and to improve mechanical properties of materials [18]. Margevicius and Lewandowski [19–21] and Margevicius *et al.* [22] recently investigated the effects of hydrostatic pressure on the flow stress and ductility of polycrystalline NiAl. They found that pressurization (0.5 to 1.4 GPa)

0022–2461

significantly affects the flow behaviour of the cast, extruded or powder metallurgical NiAl. However, some conclusions from their work need to be studied further, which will be discussed later in this paper.

We recently applied a high hydrostatic and uniaxial pressure of up to 2 GPa in the reaction synthesis (HPRS) of NiAl intermetallics from elemental powders [23], which differs from both dynamic compaction of powder materials [16] and application of hydrostatic pressure on manufactured materials [19–22]. This paper represents a continuation of the reported work [23] and the emphasis is put on the study of the relation between microstructures and mechanical properties at room temperature of a near-stoichiometric HPRS NiAl and the effects of high hydrostatic pressures on the reaction sintering process, on the microstructures and mechanical properties of the NiAl.

2. Experimental procedures

Pure nickel and aluminium powders (> 99.9%) with an average size of 12 μm were mixed in a tubular-type mixer. The powder blends were nominally stoichiometric NiAl. They were cold compacted into cylindrical samples under a pressure of 300 MPa by die pressing. The green density was 71%. The sample was then put into a piston-cylinder-type apparatus of 20 mm inner diameter to perform the HPRS process. The pressure in the vessel was calibrated within an uncertainty of $\pm$ 50 MPa by obtaining the melting curve of lead, using a high temperature differential thermal analysis (DTA) method. Pyrophyllite was used as the pressure medium. The temperature of the sample during sintering was measured within $\pm$ 1 °C by a thermocouple connected directly to the sample. It was found that the synthesis of NiAl in the HPRS is very sensitive to the process parameters. In this work, a pressure of 2 GPa, a heating temperature of 500 °C and holding time of 30 min were chosen in HPRS for obtaining stoichiometric NiAl. The HPRS samples had an appearance of cylinders with a height of about 6 mm and diameter of about 5 mm.

In order to compare the mechanical properties of the NiAl manufactured using the HPRS and normal powder metallurgy process, respectively, the elemental nickel and aluminium powders mentioned above were mixed and cold compacted by die pressing under the same conditions. The samples were then prepared by hot pressure RS in a hot press furnace. Pure argon was used to protect the NiAl from oxidation. The sintering temperature, hold time and applied pressure were 1200 °C, 2 h and 33 MPa, respectively. A heating rate of 15 °C min^{-1} was used. Temperature measurements with an uncertainty of $\pm$ 5 °C were performed using a thermocouple put into the furnace close to the graphite die containing the specimen. The sintered sample was 20 mm long with 18 mm diameter. The sintered relative density was determined by a water immersion technique [14] and calculated according to the theoretical density of 5.95 g cm^{-3} for the stoichiometric NiAl [3].

The microstructures of the HPRS NiAl were investigated using optical microscopy and Jeol 2000FX transmission electron microscopy (TEM) at 200 kV and that of the hot-pressed RS NiAl was examined using only optical microscopy. The microstructures of the specimens of both HPRS NiAl and hot-pressed RS NiAl observed by optical microscopy were revealed by immersion in a solution consisting of 20 ml HCl, 20 ml C_2H_5OH and 1 g $CuCl_2$. The sizes of the grains and dispersoids were determined using a linear intercept method. Specimens chosen for TEM examination were sectioned by cutting slices 0.2 mm thick by electrodischarge machining and polished to a thickness of about 50 μm using silicon carbide grinding papers. Disks of 3 mm diameter were then cut from the polished samples and jet-electropolished in an electrolyte of 10% sulphuric acid and 90% methanol. The microcompositional analysis was performed by means of X-ray energy dispersive spectroscopy (EDS). The uncertainty of the EDS analysis was within 2.5 at %, except for some light elements, due to employing a standard sample to improve accuracy of the measurement.

Mechanical testing in compression at room temperature of both HPRS NiAl and hot-pressed RS NiAl was performed on either an MTS Testing Machine 810 or Instron Universal Testing Machine 1195. A small right cylindrical compression specimen of 4.7 mm long (parallel to the pressing direction) with 3 mm diameter was prepared by electrodischarge machining from HPRS or hot-pressed RS samples. A constant compressive strain rate of 8.3×10^{-4} s^{-1} was used. The test data in the load–time charts were converted to true stresses and strains via an offset method [24] assuming uniform deformation and conservation of volume. The fracture surfaces of the compressive test samples were observed by means of a Hitachi S-570 scanning electron microscope (SEM). Microhardness testing of the samples was performed using a load of 100 g before observation by optical microscopy.

3. Results

3.1. Microstructures

Optical microscopy showed that the HPRS NiAl was almost fully dense, which is consistent with the measured relative density (98.2%) [23], and this is higher than the relative density (95.8%) of the hot-pressed RS NiAl. NiAl prepared by both processes consisted of a polygonal grain structure with dispersions distributed mainly on grain boundaries (Fig. 1), similar to that in RHIP NiAl and NiAl–TiB_2 [14], implying that dynamic recrystallization took place no matter whether a low or a high pressure was applied in RS. The average grain size of the HPRS NiAl was 11.2 μm, so no obvious grain growth occurred on HPRS compared to the size of the original elemental powders. However, the average grain size of the hot-pressed RS NiAl was 26.7 μm, which is more than twice the grain size of the HPRS NiAl, suggesting that grain growth occurred during hot-pressing RS. The X-ray diffraction (XRD) and EDS (in SEM) analyses [23] indicated

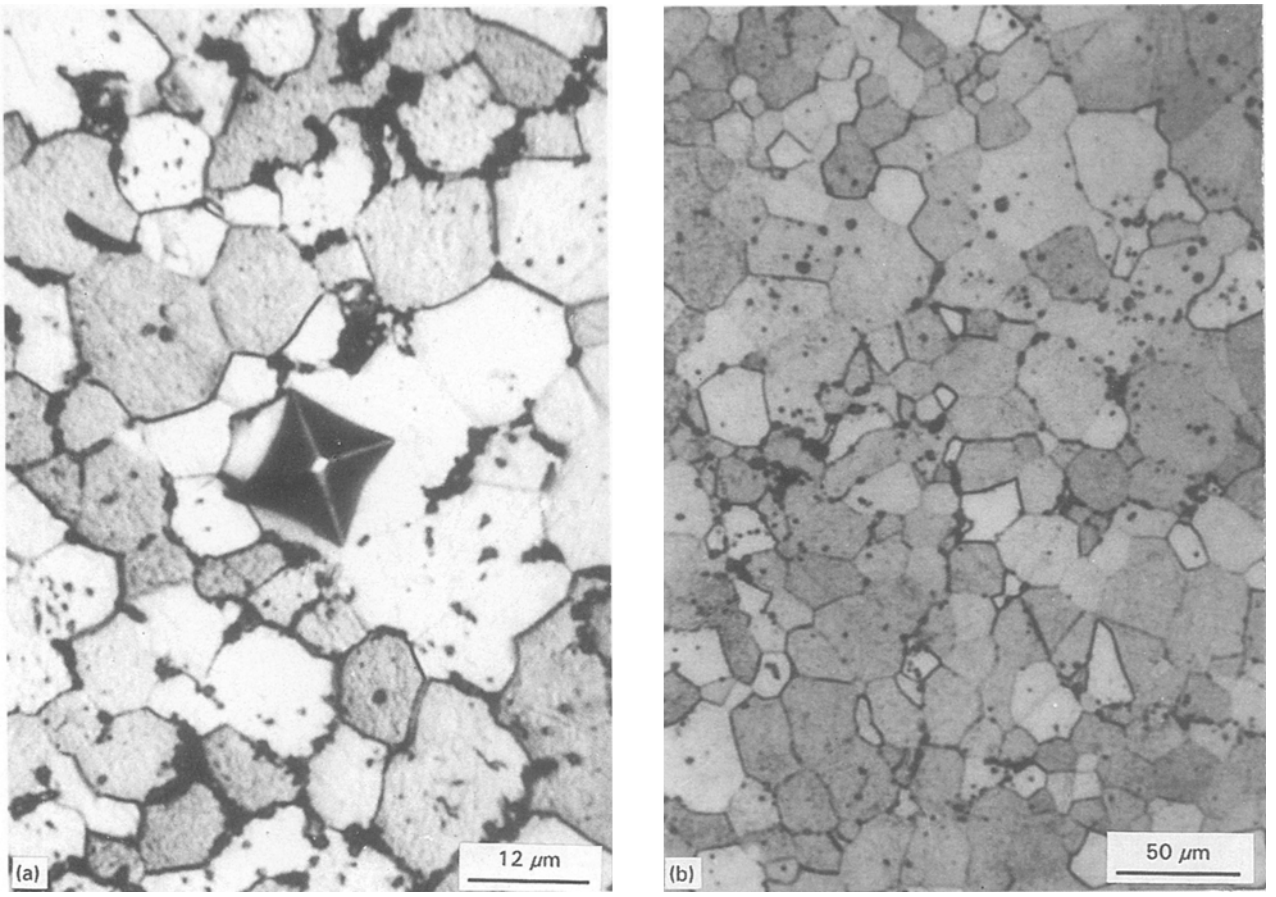

Figure 1 Microstructures (optical micrographs) (a) HPRS NiAl and (b) hot-pressure RS NiAl.

that the HPRS NiAl consisted of single phase β-NiAl with a B2 structure, in addition to aluminium-rich particles. No remaining pure nickel or aluminium was found in both XRD and EDS analyses, suggesting that the reaction between the elemental powders during HPRS was complete. A similar examination in the hot-pressed RS NiAl was performed [25], indicating that the reaction in the NiAl also was complete. The volume percentages of the aluminium-rich particles in both NiAl samples were very close and the percentage estimated is about 8.5%.

The microstructures of the HPRS NiAl were further studied by means of TEM, the results from which coincided well with the observations using optical microscopy. Selected area electron diffraction (SAED) analysis (Fig. 2) proves that the matrix of the alloy is β-NiAl. Moreover, the average size of the particles, mainly on the grain boundaries, was very small, only 0.1 μm, although agglomeration to some extent was observed using optical microscopy (Fig. 1). Additional SAED investigation revealed that the aluminium-rich particles are Al_2O_3 (Fig. 3). The microcompositional examination of the particles using EDS in TEM is consistent with the SAED analysis (Fig. 4a). The average composition of the β-NiAl grains was Ni–49.2 at % Al (Fig. 4b), which coincides with the EDS examination in SEM (Ni–48.9 at % Al [23]) within the uncertainty range. The aluminium content of the matrix is a little lower than the nominally stoichiometric NiAl due to the existence of the Al_2O_3 particles in the HPRS NiAl, which probably came from the original aluminium powders. No voids or microcracks were found around the interface between the Al_2O_3 particles and the β-NiAl matrix, suggesting that the interface bonding is very good, even under the extremely high pressure (2 GPa) during HPRS. The average size, 0.5 μm, of the Al_2O_3 particles in the hot-pressed RS NiAl was larger than that in the HPRS NiAl.

One of the significant characteristics of the HPRS NiAl is that many dislocations were present. The dislocations were distributed not only among the Al_2O_3 particles, which resulted in networks (Fig. 5a and b), and on grain boundaries (Fig. 2a and c) but also in grains (Fig. 5c). The average dislocation density measured by a normal method [26] was about 3.5×10^9 cm^{-2} but no obvious dislocation cell structure was observed. The dislocation distribution was generally homogeneous from grain to grain and within grains, which is different from the results found in pressurized NiAl [21]. Burgers vectors of dislocations different from the normal ⟨100⟩ vector in NiAl [1, 2] have not been found.

3.2. Mechanical properties

The true compressive stress–strain curves of both HPRS NiAl and hot-pressed RS NiAl are presented in Fig. 6. Both samples exhibited no obvious yield behaviour and showed significant work hardening. This similarity between HPRS and hot-pressed RS NiAl suggests that the extreme increase of the pressure on

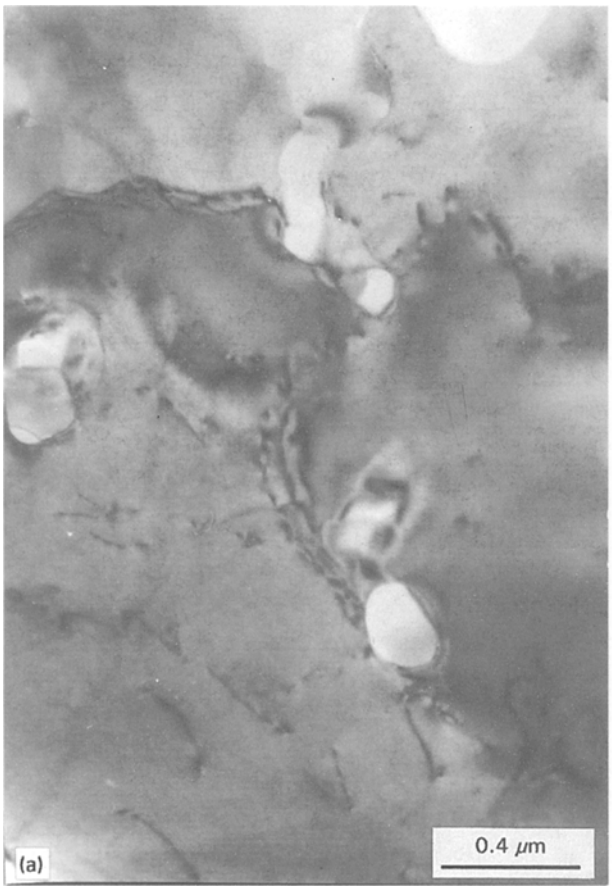

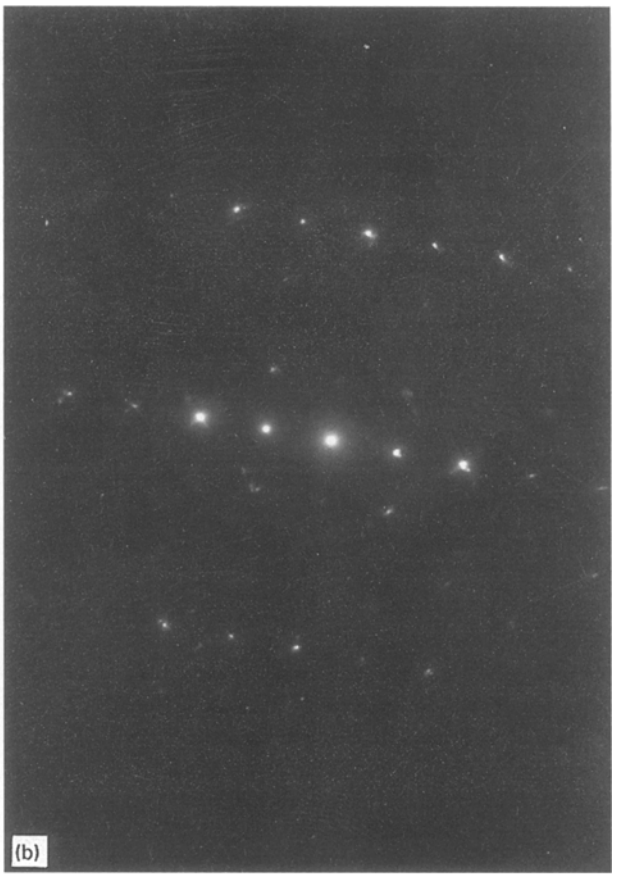

Figure 2 TEM micrographs of HPRS NiAl (a) bright field, (b) selected area electron diffraction (SAED) pattern of the matrix, β-NiAl [0 1 3] zone and (c) dark field of β-NiAl corresponding to (a).

RS did not change the flow behaviour of the NiAl in some aspects. The 0.2% offset yield strength of HPRS and hot-pressed NiAl were close to each other, 526 and 567 MPa, respectively. The yield strength of the HPRS NiAl is within the range of previous work performed on cast NiAl (311 MPa) [27], RS NiAl (544 MPa), and RHIP NiAl (890 MPa) [13]. The microhardness (H_v) of the β-NiAl in the hot-pressed RS NiAl was 287 $kg\,mm^{-2}$, which is close to the results obtained for RHIP NiAl (277 $kg\,mm^{-2}$) [14] but lower than that for HPRS NiAl (408 $kg\,mm^{-2}$). This difference probably relates to high residual stress in HPRS NiAl and the lower sintering density of the hot-pressed RS NiAl.

However, the fracture strain of the HPRS NiAl, 14.5%, was fairly high and that of the hot-pressed RS NiAl was very low, only 2.8%, this being consistent with that of NiAl fabricated using cast or normal powder metallurgy processes [1, 2]. The increase of the ductility of the HPRS NiAl is similar to the effects of the superimposed pressure in tests on the ductility of the NiAl [19] but did not induce the dramatic lowering of the yield strength as occurs with pressurized NiAl (reduced by 25%) [20, 22]. No microcracking was observed around the microhardness indents in HPRS NiAl (Fig. 1a) even under large magnification. However, it was reported [28] that the cracks were present around the microhardness indents in an annealed NiAl fabricated by mechanical alloying. Consequently, this suggests that toughness of the HPRS NiAl is good.

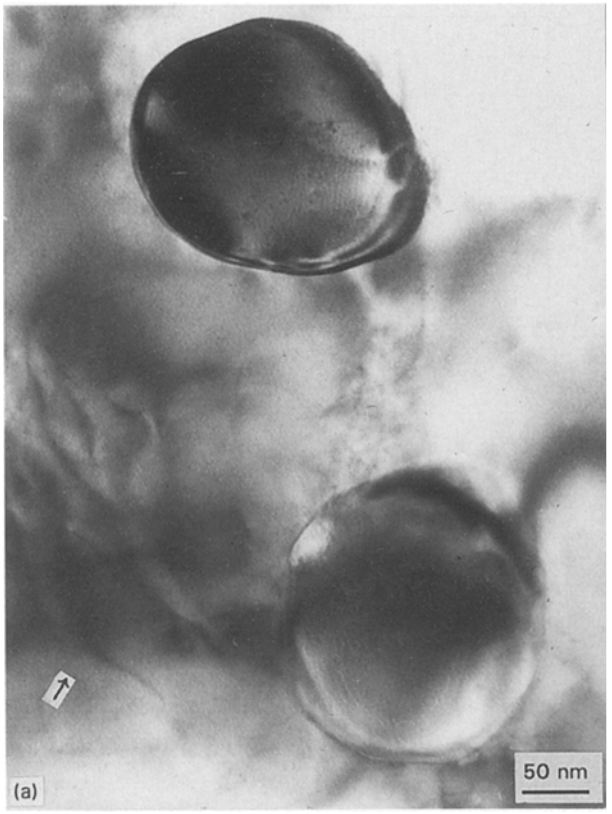

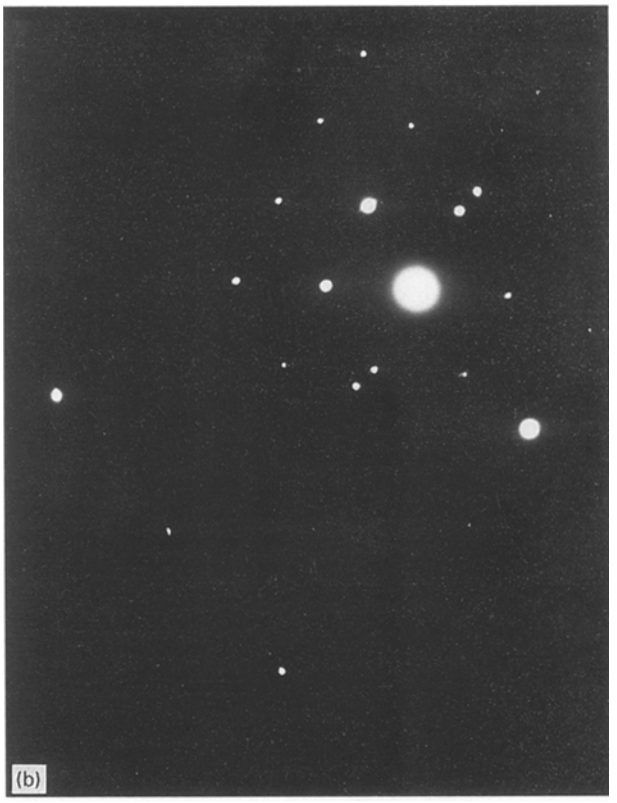

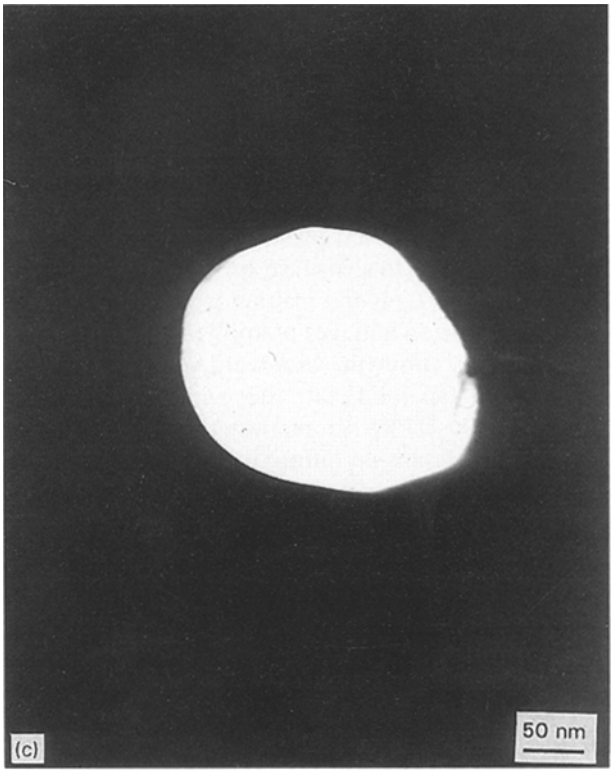

Figure 3 Identification of dispersive particles (a) particles with nanometre size and surrounding dislocations, (b) SAED patterns, Al_2O_3 [4 4 1] zone (smaller pattern) and β-NiAl [3 4 5] zone (larger pattern) and (c) dark field of the Al_2O_3 particle corresponding to (a).

3.3. Fracture surface

Compared to the brittle intergranular fracture surface of the cast NiAl [29], the fracture surface of HPRS NiAl shows a mixture of intergranular and transgranular fractures (Fig. 7a). Moreover, many deflected and branched transgranular microcracks were present on the fracture surface, suggesting again the improved toughness of the HPRS NiAl, based on our other work [5, 30]. Many very fine Al_2O_3 particles can be seen on the fracture surface. The nucleation and propagation of the microcracks did not result from the particles, which also proves the interface bonding between the Al_2O_3 particles and the β-NiAl matrix is fairly good. The fracture surface of the hot-pressed RS NiAl is shown in Fig. 7b, which shows a dominant mode of intergranular fractures. In comparison with that of HPRS NiAl and the other relevant results [5, 27], it can be deduced that intergranular fracture is difficult to avoid in NiAl if there are not sufficient independent slip systems present even though the ductility is improved to some extent.

4. Discussion

4.1. Effects of the high pressure on reaction sintering of the NiAl

Most of the powder metallurgy processes employed to fabricate intermetallics are based on reaction sintering (RS) [31]. Because of the difficulty in observing and monitoring the detailed process of RS, there has been limited understanding of RS. The study of HPRS is more difficult at this stage so we will analyse the possible mechanism for HPRS through investigation of the effects of high pressure on RS based on above experimental results.

RS generally includes two stages: one is a reactive process between the elemental powders to produce intermetallic compounds, which is also beneficial for the consolidation of the powders, and the other is a further densification process. The first process proceeds mainly through the formation of a transient

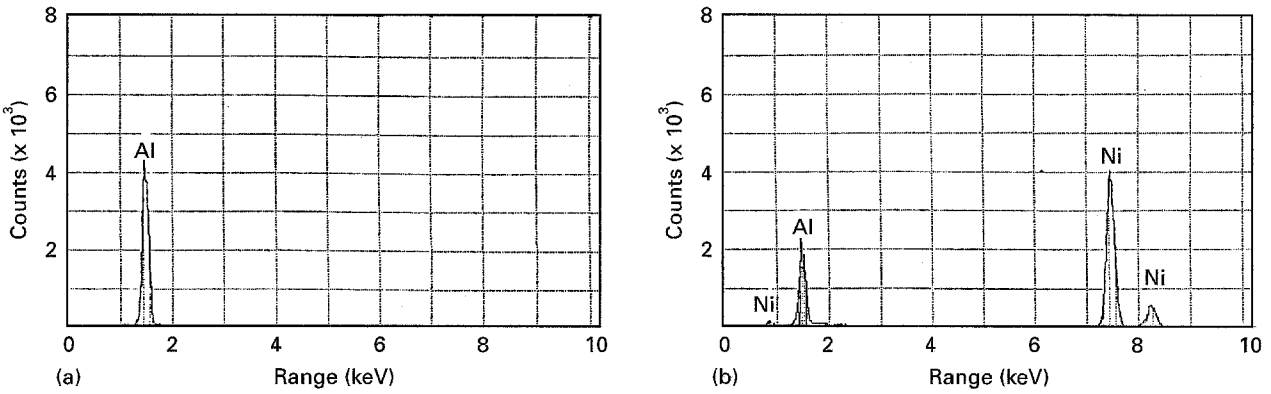

Figure 4 EDS patterns of HPRS NiAl examined with TEM (a) Al_2O_3 particle and (b) β-NiAl matrix.

liquid phase, typically a eutectic liquid, with the exotherm at the interface between contacting particles [32] in order to accelerate the reactive process, followed by consolidation. Hence, heating the compact to its lowest eutectic temperature is normally necessary in the first stage of RS [14]. For degassing and densifying through solid state diffusion of the atoms, the compact needs to be heated to a higher temperature in the second stage of RS.

In the Ni–Al binary system, the lowest eutectic temperature is about 640 °C according to the Ni–Al phase diagram [33]. Most published work indicates that the reaction temperature in RS or hot-pressed RS NiAl is about 700 °C, this being close to the lowest eutectic temperature. The density of the products with the shrinkage porosity was not high so the following consolidation by HIP, RHIP or annealing at higher temperatures (1200–1300 °C) for a long time (1–6 h) was necessary [14, 34] even for Ni_3Al [35]. The hot-pressed RS can normally combine these two stages but needs a higher heating temperature and longer hold time. In the present work, similar processing parameters (1200 °C, 33 MPa and 2 h) were applied to fabricate NiAl by hot-pressing RS: we tried unsuccessfully to lower the sintering temperature with other parameters being fixed.

Comparing the experimental results employing HPRS with those applying the normal hot-pressure RS in the fabrication of NiAl, the major characteristics of the HPRS process are: (a) applying a very high uniaxial compressive pressure, (b) employing a lower sintering and densifying temperature, and (c) without additional densification and homogenization at higher temperature. The high pressure (2 GPa) applied in the HPRS NiAl is more than 60 times that employed in the hot-pressed RS NiAl and is certainly larger than the yield strength, σ_y, of elemental powders. In fact, σ_{y1}, the yield strength of a cold-worked sample of most materials at room temperature, is less than 1.5 GPa [36]. Hence, the Al_2O_3 film on aluminium powders is easily broken into small pieces when heavy plastic deformation and severe friction result from applying the high uniaxial pressure, which is beneficial for the endothermal reduction and also is a prerequisite for the initiation of the reaction between the nickel and the aluminium. Hence, the role of the high pressure is important for lowering the reaction temperature, although the reduction was not complete in the present HPRS NiAl, which led to very fine (0.1 mm) Al_2O_3 particles being observed. The pressure applied in normal hot-pressure RS process can also play a similar role, but the pulverization effects are not apparent although the temperature is much higher, which can be seen from the larger size (0.5 mm) of the Al_2O_3 particles in the hot-pressed RS NiAl.

Compared with production of a liquid phase for accelerating the reaction in RS and normal hot-pressure RS (Fig. 8), applying a very high uniaxial pressure P ($P > \sigma_{y1}$) is an alternative way to promote the reaction. The high pressure gradient directed from powders to pores or clearances can induce heavy plastic deformation in the compact, which could play a similar role of filling the pores and increase the contact surfaces between powders (Fig. 8). It was shown [37], in fact, that plastic flow makes a significant contribution to densification of the compact at $T < T_m$, where T_m is the melting temperature of the material. These advantages of applying high pressure in HPRS may offset the disadvantages of the lower diffusivity in the solid state (no evidence of melting observed in the HPRS sample) and the negative effects of the high pressure on diffusivity. It is apparent that as soon as the condition to form NiAl is met, in some places in the compact the heat released by the reaction will accelerate the diffusion and reaction in the remaining places since the formation heat of stoichiometric NiAl, about 72 kJ mol^{-1}, is very large [2]. Consequently, employing the high pressure in HPRS can reduce the reaction temperature (500 °C for NiAl) below that of the eutectic reaction. We recently reported the formation of cold-sintered blocks of single β-NiAl phase of macroscopic size by mechanical alloying (MA) of the elemental powders [11]. The reactive process between the nickel and aluminium powders should be similar to that in HPRS but a large and repeated dynamic impact stress acted on the powders accompanied by heating from the compaction, which lead to a temperature increase estimated to be below about 100 °C. Moreover, the size of the blocks is smaller and the relative density is lower compared to the HPRS samples, which can be a reason for formation of the NiAl blocks without additional heating. The results support the above analysis of the effects of pressure on the reaction in the synthesis of NiAl.

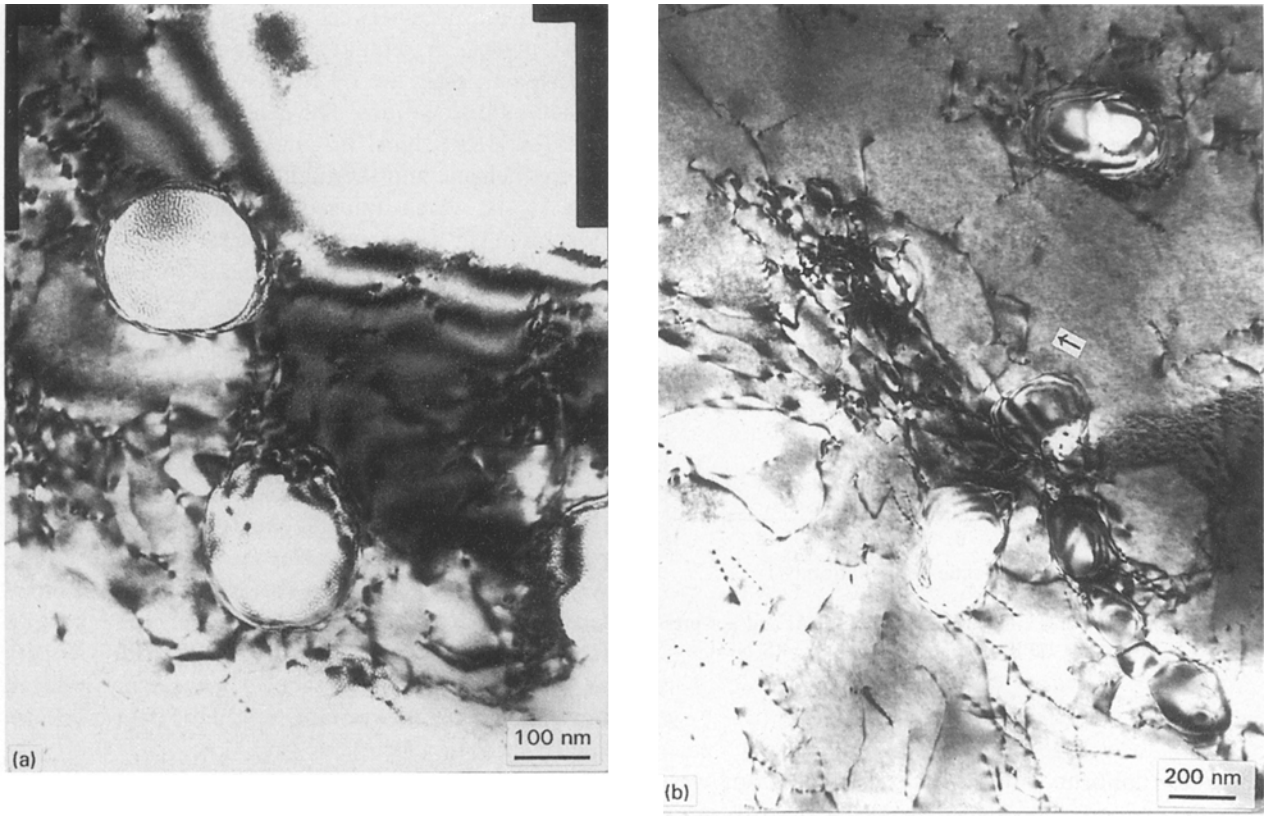

Figure 5 Dislocations in HPRS NiAl (a) dislocation networks among Al_2O_3 particles, (b) dislocations bowing out the networks (marked by arrows) and dislocation generation from interfaces between the particle and matrix and (c) dislocations with a high density within the grain.

Further study in distinguishing the effects of the stress mode (uniaxial or compressive, isostatic or dynamic) on the RS of NiAl intermetallics is necessary. Moreover, heating to a certain temperature is important to assure sufficient diffusion for completing the reaction between nickel and aluminium powders in HPRS, since one sample heated to only 400 °C (whilst keeping the other parameters constant) showed incomplete reaction.

Regarding the second stage, i.e. densification, since densifying the compact to a certain extent dominates the initiation and continuance of the reaction, depending only on solid state diffusion, the reaction process in HPRS is closely linked with the densification process (Fig. 8). On the other hand, the very high pressure and resulting plastic flow are beneficial for further densification to enhance the sintering density for shorter hold times, as shown in the experimental results. The results of the cold sintering of pure metals with a high density (> 95%), such as Al, Cu, Ni and Ti, under a high compressive pressure up to 10 GPa at room temperature were previously reported [36]. The resulting advantages from HPRS of avoiding grain growth and increasing the sintering density are apparent.

4.2. Effects of high pressure on the dislocation generation and ductility

The dislocation density is normally very low, only 1.8×10^8 cm^{-2} in cast, extruded and annealed polycrystalline NiAl [21], extremely low in polycrystalline NiAl extruded in the range of 1200 to 1400 K [29] and in annealed single-crystal NiAl [22]. Consequently, one of the effects of applying high pressure in RS of NiAl appears to be a significant increase in the dislocation density, reaching 3.5×10^9 cm^{-2} as shown in Figs 3–5. The overall dislocation distribution was

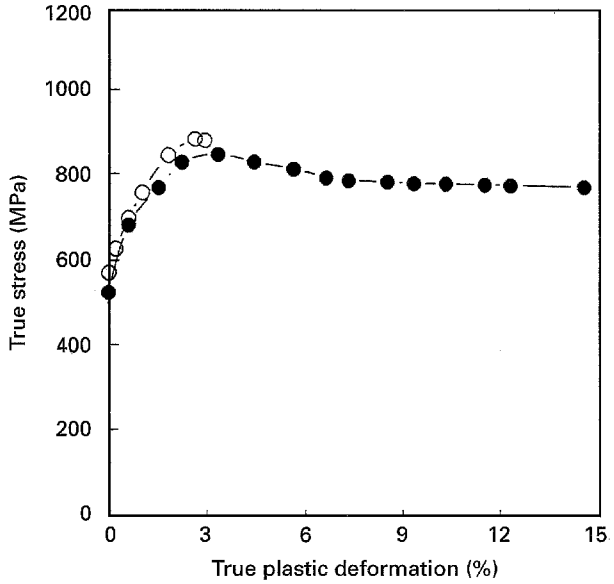

Figure 6 Compressive testing curves of HPRS NiAl and hot-pressure RS NiAl. Key: ● HPRS NiAl; ○ hot-pressure RS NiAl.

generally uniform, although more dislocations were present around the Al_2O_3 particles on the grain boundaries. It was previously pointed out [18, 21] that pressurization can generate mobile dislocations around second phase particles and inclusions in a material due to a local shear stress resulting from the differences in compressibilities, but the size of the second phase in the b c c metals should normally be smaller than 1 μm. The experimental results in the present work, including the smaller average size of the Al_2O_3 particles, less than 1 μm, is similar to that in the pressurized NiAl, although dislocation distribution is different as mentioned above. As shown in the upper right of Fig. 5b, many dislocations were generated from the interface between the Al_2O_3 particles and the NiAl matrix. A similar situation occurred around other particles in the HPRS NiAl resulting in a high density of dislocations. The generation of the dislocations in HPRS NiAl originates essentially from the different elastic and thermal properties between NiAl and Al_2O_3, which induced different elastic deformation or misfit strain between them when the HPRS NiAl was cooled to room temperature and the high pressure was removed. However, as shown in the experimental results, the interface bonding between the NiAl matrix and Al_2O_3 particles was very good, indicating that the deformation on the two sides of the interface was compatible. The misfit strain and the requirement of the compatible deformation can result in a stress concentration around the interface between the NiAl matrix and Al_2O_3 particles, which operates potential dislocation sources around the interface. A similar phenomenon was observed around the interface between NiAl and Ni_3Al in nickel-rich NiAl [7]. Estimation of the pressure-induced dislocation density in the HPRS NiAl is made. The pressure-induced misfit strain $\Delta\varepsilon_1$ between the NiAl and Al_2O_3 particles can be indicated as

$$\Delta\varepsilon_1 = \varepsilon_{1m} - \varepsilon_{1p} = \sigma(1/E_m - 1/E_p) \quad (1)$$

where E is the Young's modulus, σ is the external stress, i.e. applied pressure here. The subscripts m and p indicate the NiAl matrix and Al_2O_3 particles, respectively. Here only a linear elasticity and an approximate isostatic stress during HPRS are considered. A thermal misfit strain $\Delta\varepsilon_2$ on cooling to room temperature should be

$$\Delta\varepsilon_2 = \varepsilon_{2m} - \varepsilon_{2p} = (\alpha_m - \alpha_p)(T_2 - T_1) \quad (2)$$

where α is the coefficient of thermal expansion (CTE), T_2 is the sintering temperature and T_1 is room temperature. Hence, the pressure-induced increase of the

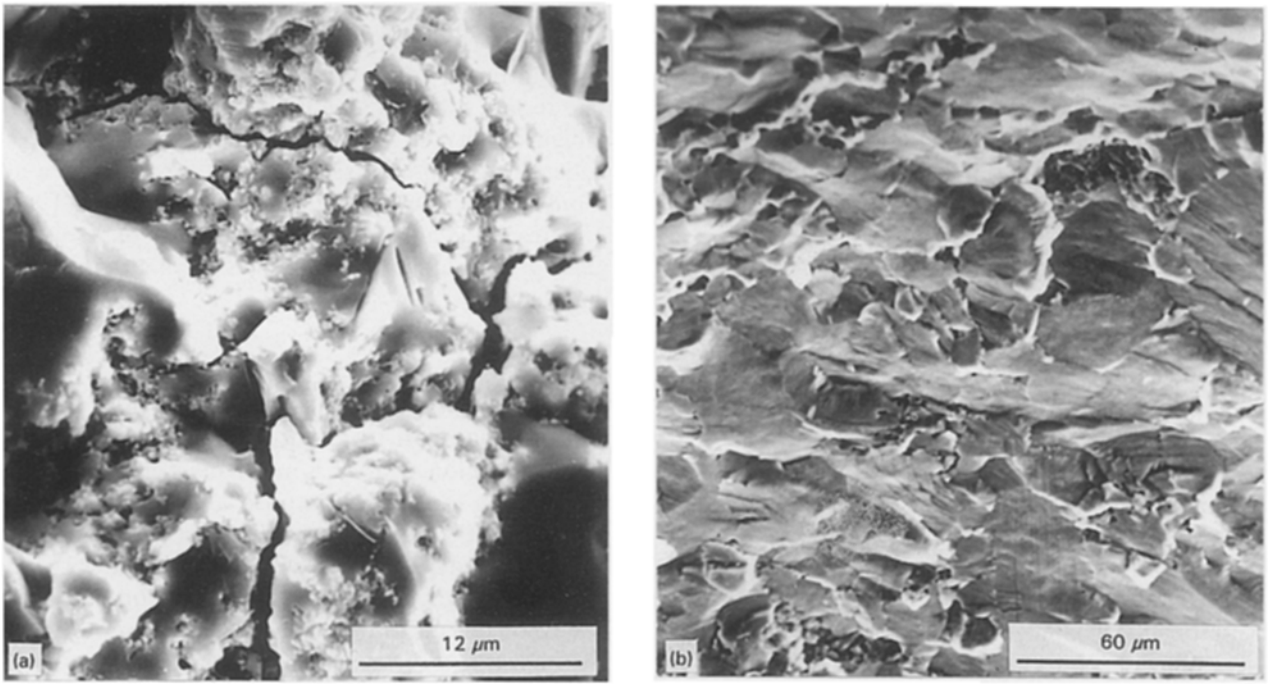

Figure 7 Compressive fracture surfaces (a) HPRS NiAl and (b) hot-pressure RS NiAl.

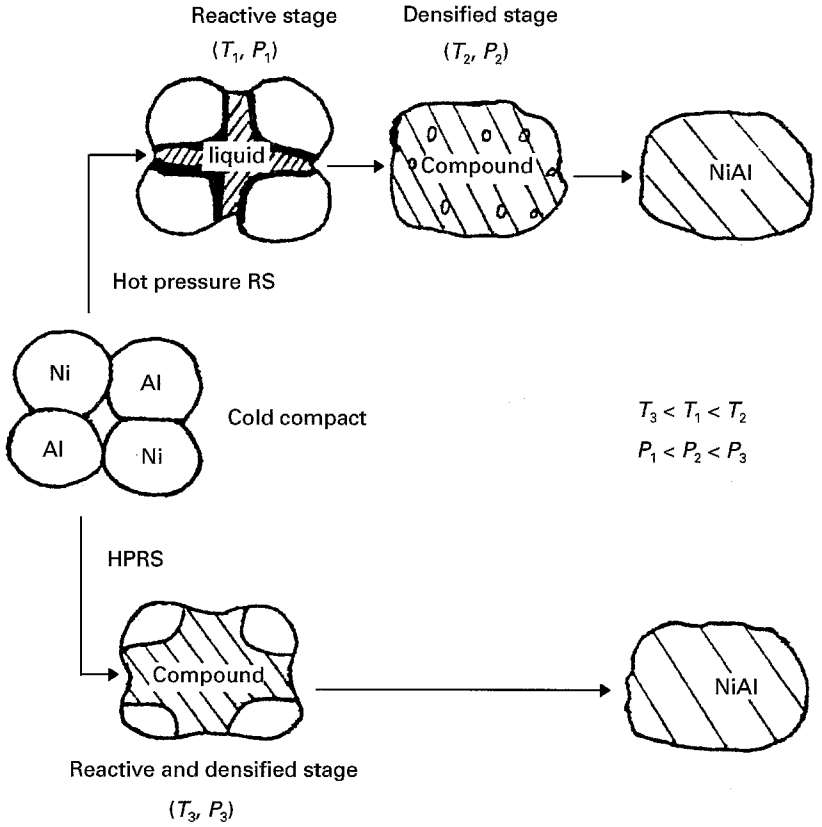

Figure 8 Schematic diagram comparing HPRS and hot-pressure RS in the synthesis of NiAl.

dislocation density $\Delta\rho$ is related to the overall misfit strain $\Delta\varepsilon$ by [38]:

$$\Delta\rho = \frac{\Delta\varepsilon}{L\mathbf{b}} = \frac{\Delta\varepsilon_1 - \Delta\varepsilon_2}{L\mathbf{b}} \quad (3)$$

where L is the free path of the dislocation motion, and $\mathbf{b}$ is Burgers vector of the dislocation. Consequently, using $L = 0.5\ \mu m$ (average distance between Al_2O_3 particles), $\mathbf{b} = 0.287$ nm for a normal $\langle 1\,0\,0\rangle$ slip in the NiAl, $\sigma = 2$ GPa, $E_m = 177$ GPa, $E_p = 524$ GPa [39], $\alpha_m = 16 \times 10^{-6}\ K^{-1}$, $\alpha_p = 9.1 \times 10^{-6}\ K^{-1}$, $T_2 = 773$ K, $T_1 = 298$ K and assuming that the CTE of both NiAl and Al_2O_3 are temperature independent on cooling from 500 °C, the pressure-induced increase of the dislocation density $\Delta\rho$ can be estimated as

$$\Delta\rho = \frac{1}{L\mathbf{b}}\left[\sigma\left(\frac{E_p - E_m}{E_p E_m} - (\alpha_m - \alpha_p)(T_2 - T_1)\right)\right] = 2.93 \times 10^9\ cm^{-2} \quad (4)$$

This value of the dislocation density coincides reasonably well with the measured value of $3.5 \times 10^9\ cm^{-2}$, suggesting that the pressure-induced injection of the dislocations in the HPRS NiAl was mainly due to the different elastic properties of Al_2O_3 particles and the NiAl matrix. Regarding the proposed point of the inhomogeneous composition within a grain as the reason for pressure-induced dislocations [20, 22], the composition in the cast and powder metallurgy alloys is generally inhomogeneous due to the segregation in the cast alloy and insufficient mixing in the powder metallurgy alloy, respectively. Moreover, the composition change within a grain is usually gradual except for the possible sudden change around the grain boundary or interface associated with various defects, substructure and second phases. Hence, the stress concentration to some extent necessary to operate the potential dislocation source around the various interfaces resulting from the high pressure and different elastic properties (also related to the composition change cross the interface instead of within a grain), should be the major reason for the generation of dislocations.

The essence of the poor ductility at room temperature of the ordered NiAl is a very complicated issue. This relates to many factors at different structural levels, such as the atomic bonding, the mobile dislocation density (associated with the dislocation structure, Pierls–Nabarro force, the dislocation generation mechanism, the antiphase boundary (APB) energy or stacking fault energy), the critical resolved shear stress (CRSS) and independent slip systems (in polycrystalline NiAl). The lack of mobile dislocations due to the high ordering energy is, at least, one of the major reasons for the low ductility of NiAl, as pointed out previously [40]. Since no new slip system was found in the HPRS NiAl, pressure-induced dislocations with a high density should contribute substantially to the improvement of the ductility in the HPRS NiAl, which was also shown in the other relevant work when high pressure was applied [36]. The residual stress in the HPRS NiAl can also contribute to the improvement of the ductility by suppression of the initiation or propagation of microcracks. It should be pointed out that the stress state in the compressive test is not as severe as that in the tensile test, so microcracks in the compressive test are not easier to propagate intergranularly as shown in [29]. Hence, simply using the

fracture strain in compressive testing as the ductility and simply comparing between compressive strain and relevant tensile properties of a material or between different materials, is not adequate. However, different fracture strains of a material, manufactured by different processes in compressive tests with the same testing conditions as a relative comparison, can provide useful information to assess the relation between the ductility and manufactured process of the material, such as that between the HPRS NiAl and hot-pressed RS NiAl in the present work, and that in the other work relevant to NiAl or other intermetallics [8, 10, 19, 41], particularly when the available sample size is limited. A detailed quantitative study to compare the effects of the compressive stress to that of the tensile stress on the ductility and strength related to the crack propagation and future application in NiAl is necessary. Efforts to manufacture HPRS NiAl with a larger size to examine the tensile properties is being carried out.

4.3. Effects of high pressure on the yield strength

A marked lowering of the yield strength (25% or about 60 MPa) in NiAl simply exposed to 500 MPa pressure was previously reported [19] and the reason was postulated to be due to pressure-induced dislocation generation. However, the yield strength of the HPRS NiAl did not decrease significantly in comparison with that of the hot-pressure RS NiAl.

Hirsch [42] proposed that the magnitude of the flow stress in an alloy with a given dislocation distribution can be attributed to a number of different contributions, such as the passing stress of two parallel dislocations of opposite sign on parallel glide planes, the long-range stress from dislocation pile-ups, the stress to operate a Frank–Read source, the stress to overcome attractive or repulsive interaction with forest dislocations, etc. Similar to dividing the flow stress into a temperature-dependent part and a temperature-independent part by Seeger [43], it can be assumed that the flow stress τ proposed by Hirsch consists of the stress τ_d to operate the dislocation sources for the dislocation generation and the stress τ_m to overcome various resistances of the other dislocations or particles to the dislocation motion i.e.

$$\tau = \tau_d + \tau_m \quad (5)$$

Hence, since the mobile dislocation density in the NiAl is normally very low, if the pressure-induced dislocations in NiAl are sufficient for the initiation of plastic deformation with an increase of the pressure, the pressure-induced decrease of the yield strength should be τ_d in Equation 5, which is difficult to calculate but is about 60 MPa in the case of the pressurized NiAl [19]. On the other hand, the pressure-induced dislocations also played a significant strengthening role in the HPRS NiAl through the reaction with the Al_2O_3 particle and their mutual reaction. It can be seen from Figs 5b and 3a (marked by arrows) that some dislocations bowed out from the networks, suggesting an Orowan strengthening mechanism. Consequently, there is a competition between the strengthening role and weakening role of the pressure-induced dislocations in NiAl. The increase of the yield stress σ_s due to Orowan strengthening can be estimated as [44]:

$$\Delta\sigma = \frac{G\mathbf{b}}{2\pi L}\ln\left(\frac{0.89r}{\mathbf{b}}\right) = 40.2\ \text{MPa} \quad (6)$$

where G is the shear modulus of the matrix, L is the interparticle spacing, r is the particle size and using $G = 76.7$ GPa [2], $L = 0.5$ μm and $r = 0.1$ μm. It is clear that the strengthening role of the pressure-induced dislocations in the HPRS NiAl can offset almost totally the weakening role if the other strengthening contributions of the dislocations through their mutual reactions, etc. are considered. This can be the reason why the yield strength of the HPRS NiAl was not significantly reduced. If the interparticle spacing in Equation 6 can be reduced or the volume fraction of the particulate can be increased, the yield strength of the HPRS NiAl would be increased, which was found in mechanical alloying of NiAl [10]. In addition, the Al_2O_3 particles with the fine size, homogeneous distribution and good bonding with the matrix, affect considerably the mechanical properties of the HPRS NiAl, although the Al_2O_3 only came from the elemental aluminium powders. The result suggests that the HPRS NiAl-based composite should show better mechanical properties if more appropriate ceramic particles are added into the NiAl.

Most of all, the HPRS process exhibits many advantages and a potential to manufacture other intermetallics and brittle materials, particularly for nanostructural materials. However, enhancing the product size, finding the relation among the processing parameters, microstructures and mechanical properties of the HPRS materials and exploring the detailed mechanism are the challenges for future study. The tensile properties at room temperature, the high temperature properties and annealing effects of the HPRS NiAl also need to be investigated further.

5. Conclusions

1. A new HPRS process was successfully employed to synthesize Ni–49.2 at % Al with a relative density of 98.2% and average grain size of 11.2 μm. The HPRS NiAl consisted of a single β-NiAl phase containing Al_2O_3 particles with an average size of 0.1 μm, distributed mainly on the NiAl grain boundaries. The application of a high uniaxial and hydrostatic compressive pressure up to 2 GPa in reaction sintering significantly reduced the sintering temperature from 1200 to 500 °C and the hold time from 1–2 h to 0.5 h in comparison with the normal hot-pressed NiAl, so that grain growth during sintering could be suppressed. The postulated HPRS process and effects of the high pressure on reaction and densification are discussed.

2. Many pressure-induced dislocations with a high density of about 3.5×10^9 cm^{-2} and generally homogeneous distribution were found in the HPRS NiAl.

The dislocations were generated from the interface between the Al_2O_3 particles and the β-NiAl matrix. The phenomenon was assumed to be due mainly to the different elastic properties between the dispersoid and the matrix and the requirement for compatible deformation on removing the high pressure. The quantitative estimation of the pressure-induced dislocation density based on this assumption is reasonably consistent with the measured results. The significant improvement of the compressive ductility (14.5%) of the HPRS NiAl was achieved in comparison with the low fracture strain (2.8%) of the normal hot-pressed RS NiAl under the same testing condition. No new slip system was identified and the fracture surface of the HPRS NiAl showed a mixture transgranular fracture and intergranular fracture modes. Hence, the pressure-induced dislocations were considered to be the major reason for the improvement of the ductility in the HPRS NiAl.

3. The yield strength (526 MPa) of the HPRS NiAl is close to that of the hot-pressed RS NiAl (567 MPa), indicating that the pressure-induced dislocations hardly affected the yield strength of the NiAl. The strengthening and weakening roles of the pressure-induced dislocations are discussed. The quantitatively estimated values for the two effects suggest that the strengthening role of the pressure-induced dislocations can offset almost totally their weakening role on the yield strength of the HPRS NiAl.

Acknowledgements

The author wishes to thank the Chinese Natural Science Foundation for the financial support.

References

1. D. B. MIRACLE, *Acta Metall. Mater.* **41** (1993) 649.
2. R. D. NOEBE, R. R. BOWMAN and M. V. NATHAL, *Int. Mater. Rev.* **38** (1993) 193.
3. R. DAROLIA, D. F. LAHRMAN, R. D. FIELD, J. R. DOBBS, K. M. CHANG, E. H. GOLDMAN and D. G. KONITZER, in "Ordered Intermetallics-Physical Metallurgy and Mechanical Behavior", edited by C. T. Liu, R. W. Cahn and G. Sauthoff (Kluwer Acad., Netherlands, 1992) p. 679.
4. R. DAROLIA, in "Structural Intermetallics", edited by R. Darolia, J. J. Lewandowski, C. T. Liu, P. L. Martin, D. B. Miracle and M. V. Nathal (TMS, Warrendale, 1993) p. 755.
5. TIANYI CHENG, M. H. FLOWER and M. MCLEAN, *Scripta Metall. Mater.* **26** (1992) 1913.
6. D. R. PANK, M. V. NATHAL and D. A. KOSS, *J. Mater. Res.* **5** (1990) 942.
7. TIANYI CHENG, *Scripta Metall. Mater.* **30** (1994) 331.
8. J. D. WHITTENBERGER, in "Structural Intermetallics", edited by R. Darolia, L. L. Lewandowski, C. T. Liu, P. L. Martin, D. B. Miracle and M. V. Nathal, (TMS, Warrendale, 1993) p. 819.
9. TIANYI CHENG, *Scripta Metall. Mater.* **27** (1992) 771.
10. M. DOLLAR, S. DYMEK, S. J. WHANG and P. NASH, *Metall Trans.* **24A** (1993) 1993.
11. TIANYI CHENG, *Scripta Metall. Mater.* **31** (1994) 1599.
12. D. A. KOSS, in Proceedings of the 2nd International Conference on Mechanical Alloying for Structural Application, edited by deBarbadillo, F. H. Froes and R. Schwarz (American Society for Metals International, Materials Park, OH, 1993) p. 281.
13. S. SAMPATH, R. TIWARI, B. GUDMUNDSSON and H. HERMAN, *Scripta Metall. Mater.* **25** (1991) 1425.
14. D. E. ALMAN and N. S. STOLOFF, *Int. J. Powder Metall.* **27** (1991) 29.
15. N. S. STOLOFF and D. E. ALMAN, *MRS Bull.* **12** (1990) 47.
16. TIANYI CHENG and SHOUHUA ZHANG, "Rapid Solidification Technology and Advanced Materials", (Chinese Aerospatial Pub., Beijing, 1990).
17. B. VODAR and Ph. MARTEAU, "High Pressure Science and Technology" (Pergamon, Oxford, 1980).
18. H. LI. D. PUGH, "The Mechanical Behavior of Materials Under Pressure" (Elsevier, Amsterdam, 1970).
19. R. W. MARGEVICIUS and J. J. LEWANDOWSKI, *Scripta Metall. Mater.* **25** (1991) 2017.
20. *Idem, ibid.* **26**, (1992) 1733.
21. *Idem, Acta Metall. Mater.* **41** (1993) 485.
22. R. W. MARGEVICIUS, J. J. LEWANDOWSKI and I. E. LOCCI, in "Structural Intermetallics", edited by R. Darolia, J. J. Lewandowski, C. T. Liu, P. L. Martin, D. B. Miracle and M. V. Nathal (TMS, Warrendale, 1993) p. 577.
23. TIANYI CHENG, *Scripta Metall. Mater.* **30** (1994) 247.
24. J. D. WHITTENBERGER, *Metall. Trans.* **10A** (1970) 1285.
25. TIANYI CHENG, *Chinese J. Mater. Res.* **9** (1994) 29.
26. R. K. HAM, *Phil. Mag.* **6** (1961) 1183.
27. E. M. SCHULSON and D. R. BARKER, *Scripta Metall.* **17** (1983) 519.
28. P. NASH, S. C. UR and M. DOLLAR, in Proceedings of the 2nd International Conference on Mechanical Alloying for Structural Application, edited by J. J. deBarbadillo, F. H. Froes and R. Schwarz (American Society for Metals International, Materials Park, OH, 1993) p. 367.
29. R. R. BOWMAN, R. D. NOEBE, S. V. RAJ and I. E. LOCCI, *Metall. Trans.* **23A** (1992) 1493.
30. TIANYI CHENG, *J. Mater. Sci.* **28** (1993) 5909.
31. A. BOSE, B. H. RABIN and R. M. GERMAN, *Powder Metall. Int.* **20** (1988) 25.
32. R. M. GERMAN, "Liquid Phase Sintering" (Plenum, New York, 1985).
33. T. MASSALSKI, "Binary Alloy Phase Diagram" (American Society for Metals, Metals Park, OH, 1986).
34. R. M. GERMAN, A. BOSE, J. MURRAY, P. KARINKO, R. ODDONE and N. S. STOLOFF, in "Powder Metallurgy '90" (The Institute of Metals, London, 1990) p. 310.
35. C. NISHIMURA and C. T. LIU, *Acta Metall. Mater.* **41** (1993) 113.
36. E. Y. GUTMANAS, A. RABINKIN and M. ROITBERG, in "High Pressure Science and Technology", edited by B. Vodar and Ph. Marteau (Pergamon, Oxford, 1980).
37. D. S. WILKINSON and M. F. ASHBY, *Acta Metall.* **23** (1975) 1277.
38. R. J. ARSNAULT and R. M. FISHER, *Scripta Metall.* **17** (1983) 67.
39. D. M. SHAN and D. L. ANTON, in "Structural Intermetallics", edited by R. Darolia, L. L. Lewandowki, C. T. Liu, P. L. Martin, D. B. Miracle and M. V. Nathal (TMS, Warrendale, 1993) p. 755.
40. R. DAROLIA, *JOM* **44** (1991) 43.
41. D. P. POPE and F. CHU, in "Structural Intermetallics", edited by R. Darolia, L. L. Lewandowski, C. T. Liu, P. L. Martin, D. B. Miracle and M. V. Nathal (TMS, Warrendale, 1993) p. 637.
42. P. B. HIRSCH, "The Physics of Metals", Vol. 2 (Cambridge University Press, Cambridge, 1975) p. 175.
43. A. SEEGER, in "Dislocations and Mechanical Properties of Crystals", edited by J. C. Fisher (John Wiley, New York, 1957) p. 243.
44. M. F. ASHBY, in "Oxide Dispersion Strengthening", edited by G. S. Ansell (Gordon and Breach, New York, 1968) p. 143.

Received 22 May
and accepted 4 October 1995